Control of multidimensional integrable Hamiltonian systems

C. W. Kulp
Department of Physics and Astronomy, Eastern Kentucky University, Richmond, Kentucky 40475, USA

E. R. Tracy
Department of Physics, The College of William & Mary, Williamsburg, Virginia 23187-8795, USA
(Received 12 November 2004; published 20 September 2005)

In this paper, we study the controllability of a four-dimensional integrable Hamiltonian system that arises as a low-mode truncation of the nonlinear Schrödinger equation [Bishop *et al.*, Phys. Lett. A **144**, 17 (1990)]. The controller targets a solution of the uncontrolled dynamics. We show that in the limit of small control coupling, a Takens-Bogdanov bifurcation occurs at the control target. These results support our earlier claim that Takens-Bogdanov bifurcations will generically occur when dissipative control is applied to integrable Hamiltonian sytems. The presence of the Takens-Bogdanov bifurcation causes the control to be extremely sensitive to noise. Here, we implement an algorithm first developed in Kulp and Tracy [Phys. Rev. E **70**, 016205 (2004)] to extract a subcritical noise threshold for the four-dimensional system.

DOI: 10.1103/PhysRevE.72.036213 PACS number(s): 05.45.Xt, 45.20.Jj, 45.80.+r

I. INTRODUCTION

The control of Hamiltonian systems has attracted much attention over the past 20 years. While a complete list of references is too extensive to list here, we wish to briefly review some of the topics studied in the past 20 years. Much of this work has focused on controlling Hamiltonian systems that are chaotic when the control is turned off [1–7]. There are also examples of possible physical applications of this work. For example in [8], the results of [5] are used to find a chaotic Earth-Moon transfer orbit which requires a smaller velocity boost than a Hohmann transfer. The previous work most relevant to the current paper, however, deals with nonchaotic Hamiltonian systems. In [9], Haberman and Ho study a Hamiltonian system which is a nonchaotic nonlinear oscillator. The phase space of this system contains two competing centers separated by a saddle. Once a dissipative perturbation is applied to the system, the centers become attractors. In [9], asymptotic methods are used to derive an analytic form for the stable manifold of the saddle (the basin boundary between attractors). Other topics in the control of Hamiltonian systems include: controlling global stochasticity [10], the control of dissipative and Hamiltonian chaos [11], control of chaotic maps [12], the control of Hamitonian systems containing both chaotic and quasiperiodic regions of their phase space [13], and the controllability of twist maps [14]. There has also been work done in understanding the control of integrable and near-integrable systems [15–18]. Friedland and Shagalov [27] have done some work dealing with exciting N-phase solutions of the nonlinear Schrödinger equation (NLS), an integrable Hamiltonian system. In [27], a simple conservative control scheme is used to open islands around a moving control target. In our work, we focus on the control of finite-dimensional integrable Hamiltonian systems. The controller uses dissipative and conservative terms to target an exact solution of the uncontrolled system. Our long term goal is to learn how to control nonlinear waves that are well-modeled by integrable theories, hence we focus on the control of integrable Hamiltonian systems, rather than chaotic ones.

In [19] we studied the problem of controlling two-dimensional integrable Hamiltonian systems to one of their exact solutions. The controller used to target the solution of interest contained dissipative and conservative terms. The controlled system is of the form:

$$\dot{z} = J\nabla H(z) + (\epsilon_R 1 + \epsilon_I J)(z_0 - z), \tag{1}$$

where $z=z(t)$ is a $2N$-vector, H is the Hamiltonian, ϵ_R and ϵ_I are constants, 1 is the $2N\times 2N$ identity matrix, and J is the $2N\times 2N$ block matrix:

$$J = \begin{pmatrix} 0 & -1 \\ 1 & 0 \end{pmatrix}. \tag{2}$$

In J, the 0 and 1 are $N\times N$ block matrices. Further, $z_0(t)$ is a solution of the uncontrolled dyanmics ($\epsilon_R=\epsilon_I=0$) which is the target for control. The couplings ϵ_R and ϵ_I are, respectively, dissipative and conservative control terms. Equation (1) can be canonically transformed into

$$\dot{\mathbf{Z}} = J\nabla_{\mathbf{Z}} K(\mathbf{Z},t) - \epsilon_R \mathbf{Z} - \epsilon_I J S_0(t)\mathbf{Z} + O(\mathbf{Z}^2), \tag{3}$$

where Z is a coordinate system that keeps the target solution fixed at the origin. In this paper, we consider the case in which the conservative coupling is zero.

In our previous work, we studied the case in which $N=1$. We found that the dissipative term in Eq. (1) caused a Takens-Bogdanov bifurcation [23,24] to occur at the control target. The Takens-Bogdanov bifurcation implies that the controlled system will be extremely sensitive to noise. We then illustrated these results on a driven nonlinear Schrödinger equation (NLS), an integrable Hamiltonian system whose solutions were restricted to plane waves (spatially uniform solutions). In this paper, we will expand upon our earlier work to include four-dimensional systems. This time, our sample system will be a four-dimensional integrable Hamiltonian system based upon the NLS [20]. This system

will have some of the properties of the NLS, such as plane wave instability. We will find that a Takens-Bogdanov bifurcation occurs in this new system as well.

The phase space of an integrable Hamiltonian system is foliated by tori. Our target orbit lies on one such torus. By a canonical transformation, we can cast Hamilton's equations into action angle form and bring the target orbit to rest at the origin. Linearizing Hamilton's equation about the fixed point at the origin gives

$$\begin{pmatrix} \dot{\phi}_1 \\ \dot{I}_1 \\ \dot{\phi}_2 \\ \dot{I}_2 \end{pmatrix} = \begin{pmatrix} 0 & \lambda_1 & 0 & 0 \\ 0 & 0 & 0 & 0 \\ 0 & 0 & 0 & \lambda_2 \\ 0 & 0 & 0 & 0 \end{pmatrix} \begin{pmatrix} \phi_1 \\ I_1 \\ \phi_2 \\ I_2 \end{pmatrix} + \begin{pmatrix} g_1(\mathbf{I}) \\ 0 \\ g_2(\mathbf{I}) \\ 0 \end{pmatrix}. \quad (4)$$

Notice that the linear term is in Jordan block form and nondiagonalizable. Therefore it is generic that Takens-Bogdanov bifurcations will occur when controlling such systems. This paper provides further evidence for the importance of this assertion by examining an important special case: a low-mode truncation of the nonlinear Schrödinger equation that preserves the integrability of the original PDE. The analysis of the controlled dynamics of Eq. (4) is difficult due to the large number of parameters which can appear when control is applied. From Eq. (3) it is clear that the ϵ_R terms will appear on the diagonal of Eq. (4). However, the placement of the conservative terms depends on the problem at hand. This makes a general analysis difficult. In this paper we will set the conservative term, ϵ_I, equal to zero and study the effects of a purely dissipative control term on an integrable Hamiltonian system.

The work presented in this paper is a nontrivial extension of the work presented in [19]. The possibility of multiple Takens-Bogdanov bifurcations increases the difficulty of analyzing the controllability of the system. In fact, in one of the examples below, a Takens-Bogdanov bifurcation will occur in two different subspaces. This type of behavior was not previously dealt with, but here we show that a careful application of our algorithm will still yield fruitful results. Often, the Takens-Bogdanov nature of these systems will not be immediately obvious in the coordinates used to describe the system, thus obscuring the degenerate nature of the system in the physical coordinates. Using the action-angle coordinates in [19] greatly simplified the analysis of the two-dimensional control problem and made the degeneracy obvious. In many real systems, the action-angle variables are not available. In this paper, the action-angle coordinates will not be available for the analysis because, although they exist, they are not known in closed form. We will still perform the normal form analysis similar to that done before, however, a blind application of the normal form can lead to spurious roots. Further, since we do not know the action-angle coordinates, we will need to alter the method used in our earlier work. We will use the information obtained from the normal form analysis to estimate scalings in the physical coordinates. We will see that we can still obtain useful information about the controllability of the system when such an analysis is done.

A long term goal of our work is to develop controllers for systems whose dynamics reduce to the NLS in some limit. In particular, we are interested in the suppression of instabilities inherent in these types of systems. Such instabilities are represented by the theta-function solutions of the NLS presented in [21]. Effective control of the NLS to its theta-function solutions will give insight into the suppression of such instabilities. By studying the control of related higher dimensional systems (i.e., based upon the NLS) which retain the properties of the NLS, we hope to obtain some insight into the control of the NLS itself, which is an infinite dimensional problem.

II. THE UNCONTROLLED DYNAMICS

The work in this section parallels the development in [20]. We begin with the NLS, $iw_t+w_{zz}+2|w|^2w=0$, which is an infinite-dimensional integrable Hamiltonian system. Next, we transform to a coordinate system which places the plane wave solution, $w(z,t)=a\exp(2ia^2t)$, at rest (but not at the origin). This transformation is canonical [22]. By setting $w(z,t)=q(z,t)\exp(2ia^2t)$ and inserting it into the NLS, we obtain

$$iq_t + q_{zz} + 2(|q|^2 - a^2)q = 0. \quad (5)$$

Next, we consider the two-mode truncation from [20], $q(z,t)=c(t)+b(t)\cos(kz)$, where $c(t)$, the carrier, and $b(t)$, the sideband, are complex. We insert this into Eq. (5) to obtain

$$\dot{c} = 2i\left(|c|^2 + \frac{1}{2}|b|^2 - a^2\right)c + i(c^*b + cb^*)b,$$

$$\dot{b} = 2i\left[|c|^2 + \frac{3}{4}|b|^2 - \left(\frac{1}{2}k^2 + a^2\right)\right]b + 2i(bc^* + cb^*)c, \quad (6)$$

which is a two-dimensional system of complex variables (four-dimensional real system). It it is important to note that the derivation of Eq. (6) from Eq. (5) requires that we drop terms in $\cos(3kz)$ and higher harmonics. Hence this is not a solution of the NLS but a new dynamical system in its own right that was inspired by the NLS and exhibits some of its interesting features. The system (6) admits the two first integrals (see [20] and references therein):

$$I = |c|^2 + \frac{1}{2}|b|^2,$$

$$H = \frac{1}{2}|c|^4 + \frac{3}{2}|b|^2|c|^2 + \frac{1}{4}|b|^4 - \left(\frac{1}{2}k^2 + a^2\right)|b|^2 - 2a^2|c|^2 + \frac{1}{2}(b^2c^{*2} + c^2b^{*2}). \quad (7)$$

The first integrals, I and H, are independent and are in involution and therefore the system (6) is a four-dimensional integrable Hamiltonian system with phase space corrdinates, (c_I, c_R, b_I, b_R), and with Poisson bracket:

TABLE I. The solutions of Eq. (10) in (c,b) coordinates.

Circle	(c,b)	(y,x,v,u)
C1	$(ae^{i\phi},0)$	$(0,a,0,0)$
C2	$(0,e^{i\phi}\sqrt{\frac{4}{3}(a^2+\frac{1}{2}k^2)})$	$(0,0,0,\sqrt{\frac{4}{3}(a^2+\frac{1}{2}k^2)})$
C3	$(e^{i\phi}\sqrt{(k^2+a^2)/5},e^{i\phi}\sqrt{2(4a^2-k^2)/15})$	$(0,\sqrt{(k^2+a^2)/5},0,\sqrt{2(4a^2-k^2)/15})$

$$\{f,g\}=\frac{\partial f}{\partial c_I}\frac{\partial g}{\partial c_R}-\frac{\partial f}{\partial c_R}\frac{\partial g}{\partial c_I}+\frac{\partial f}{\partial b_I}\frac{\partial g}{\partial b_R}-\frac{\partial f}{\partial b_R}\frac{\partial g}{\partial b_I}, \tag{8}$$

where f,g are functions of c_I, c_R, b_I, and b_R.

For our work, we use the following set of variables:

$$c(t)=x(t)+iy(t),$$

$$b(t)=u(t)+iv(t). \tag{9}$$

In these variables, Eq. (6) becomes

$$\dot{y}=2x\left(x^2+y^2+\frac{1}{2}(u^2+v^2)-a^2\right)+2u(xu+yv),$$

$$\dot{x}=-2y\left(x^2+y^2+\frac{1}{2}(u^2+v^2)-a^2\right)-2v(xu+yv),$$

$$\dot{v}=2u\left[x^2+y^2+\frac{3}{4}(u^2+v^2)-\left(\frac{1}{2}k^2+a^2\right)\right]+4x(xu+yv),$$

$$\dot{u}=-2v\left[x^2+y^2+\frac{3}{4}(u^2+v^2)-\left(\frac{1}{2}k^2+a^2\right)\right]-4y(xu+yv). \tag{10}$$

One important property, which is of interest to us, is that plane wave solutions are modulationally unstable when $k<2a$ [21]. This will have direct consequences for controlling the NLS to the plane wave solution, $q_0=a$. The modulational instability was not a concern in the two-dimensional (plane wave) case since the system did not allow for spatially nonuniform solutions of the NLS. The modulational instability is retained in the truncated system (10), as will be shown below. The instability is associated with a saddle structure in the phase space of the uncontrolled system.

There are several special solutions of Eq. (10) presented in [20]. We are interested in using three of them as control targets. They are listed in Table I ($\phi\in[0,2\pi]$). Note that C1 is the plane wave target from [19]. As we will see, each of these solutions will be interesting control targets and will demonstrate a variety of possible behaviors that the controlled system can exhibit.

III. ANALYSIS OF THE CONTROLLED DYNAMICS

In this section, we will present the problem of controlling Eq. (10) to the solutions presented above. In this paper, we exploit the fact that the normal form analysis does not require knowledge of the action-angle coordinates. We know that Eq. (10) is integrable, and therefore from Eq. (4), we expect the Takens-Bogdanov bifurcation to occur. The analysis will be done as follows.

(1) Perform a coordinate transformation which places the target orbit at rest at the origin. Here we will truncate the dynamics at quadratic order.

(2) Next, we perform a linear coordinate transformation which places the linear dynamics from Step 1 into Jordan canonical form. We then identify the quadratic terms which are resonant to the linear dynamics by computing the normal form [25] of the system to quadratic order.

(3) Use the equations from step 2 to find the scalings (in ϵ_R) for the fixed points near the target, in the normal form coordinates.

(4) Using the scalings found in step 3, we can go back to the original equations and compute the location of those fixed points. This is a new step in the analysis. The reason for this new step will be explained below.

(5) We identify which fixed points are saddles that bifurcate with the target as $\epsilon_R\downarrow 0$.

(6) We then find the angle, θ, between the eigenvectors of the saddle which are becoming degenerate (parallel) when $\epsilon_R\downarrow 0$. This will involve one pair of stable and unstable eigenvectors becoming degenerate.

(7) Finally, we use the triangle relation, first demonstrated in [23], to estimate the noise threshold for instability denoted σ_c.

Notice that we will not be extracting σ_c directly from our normal form as done in our earlier work. The normal form can provide spurious roots when truncated to second order. We will demonstrate this on the Circle 1 problem below. The occurrence of spurious roots is one of the major reasons for the modification of the analysis and did not occur in our previous work on the two-dimensional problem.

Our controlled dynamics will be

$$iq_t+q_{zz}+2(|q|^2-a^2)q=i\epsilon_R(q_0-q), \tag{11}$$

where q_0 is a solution to the uncontrolled ($\epsilon_R=0$) dynamics, either Circle 1, 2, or 3.

A. Targetting Circle 1: C1=(y,x,v,u)=$(0,a,0,0)$

In this section we focus on the problem of controlling the truncated NLS, Eq. (10), to Circle 1, which is the plane wave solution from the two-dimensional problem presented in [19]. The four-dimensional model includes more of the physics of the NLS (i.e., the plane wave instability) and therefore makes it much more relevant to understanding the control of the NLS to a plane wave state.

We begin by substituting the two-mode truncation from above into Eq. (11), with $q_0=a$. Then we follow the procedure used to obtain Eq. (10):

$$\dot{y} = -\epsilon_R y + 2x\left(x^2+y^2+\frac{1}{2}(u^2+v^2)-a^2\right)+2u(xu+yv),$$

$$\dot{x} = \epsilon_R(a-x) - 2y\left(x^2+y^2+\frac{1}{2}(u^2+v^2)-a^2\right)-2v(xu+yv),$$

$$\dot{v} = -\epsilon_R v + 2u\left[x^2+y^2+\frac{3}{4}(u^2+v^2)-\left(\frac{1}{2}k^2+a^2\right)\right] + 4x(xu+yv),$$

$$\dot{u} = -\epsilon_R u - 2v\left[x^2+y^2+\frac{3}{4}(u^2+v^2)-\left(\frac{1}{2}k^2+a^2\right)\right] - 4y(xu+yv). \quad (12)$$

The target is located at ($y=0$, $x=a$, $v=0$, $u=0$).

Next, we shift the target to the origin and keep only the linear and quadratic terms (e.g., $x=a+X, X\ll 1$):

$$\begin{pmatrix}\dot{Y}\\ \dot{X}\\ \dot{V}\\ \dot{U}\end{pmatrix} = \begin{pmatrix}-\epsilon_R & 4a^2 & 0 & 0\\ 0 & -\epsilon_R & 0 & 0\\ 0 & 0 & -\epsilon_R & 4a^2-k^2\\ 0 & 0 & k^2 & -\epsilon_R\end{pmatrix}\begin{pmatrix}Y\\ X\\ V\\ U\end{pmatrix} + f_2(\mathbf{Y}) + \cdots, \quad (13)$$

where

$$f_2(\mathbf{Y}) = \begin{pmatrix}2a\left(Y^2+\frac{3U^2}{2}+\frac{V^2}{2}+3X^2\right)\\ -4aYX-2aVU\\ 4a(3XU+YV)\\ -4aVX-4aYU\end{pmatrix}. \quad (14)$$

The eigenvalues of the linear matrix give the stability for the target. The eigenvalues of the matrix in Eq. (13) are $-\epsilon_R$, $-\epsilon_R, -\epsilon_R \pm k\sqrt{4a^2-k^2}$. The target is a degenerate node in the xy plane. The target becomes unstable when $k<2a$, this is how the NLS's plane wave instability appears in the control problem. Further, the target is also unstable when $\epsilon_R < k\sqrt{4a^2-k^2}$. The term $k\sqrt{4a^2-k^2}$ gives the linear growth rate for modulational instabilities, hence this shows that the damping rate of the control must be greater than the linear growth rate of the instability. The problem is split in two different cases: one where the plane waves are modulationally stable and the other where they are not.

1. The case in which plane waves are modulationally stable

When $k>2a$, the target is an attractor. Therefore we can consider computing a σ_c for it. The quantity, σ_c, is the smallest perturbation that drives the system unstable (which we call the "distance" to the basin boundary). We do this by continuing with the steps outlined in Sec. III.

Next, we calculate the normal form of Eq. (13) to second order about the target when $\epsilon_R=0$. The details of this transformation are not important (the interested reader is referred to [26]), however, the relationship between the coordinates (Y,X,V,U) and the normal form coordinates (x_1,x_2,x_3,x_4) is important when finding fixed points of Eq. (12). The coordinates Y and X are proportional to x_1 and x_2, respectively; while the coordinates U and V are linear combinations of x_3 and x_4. The normal form of Eq. (13) about the target is

$$\begin{pmatrix}\dot{x}_1\\ \dot{x}_2\\ \dot{x}_3\\ \dot{x}_4\end{pmatrix} = \begin{pmatrix}-\epsilon_R & 1 & 0 & 0\\ 0 & -\epsilon_R & 0 & 0\\ 0 & 0 & -\epsilon_R-b & 0\\ 0 & 0 & 0 & -\epsilon_R+b\end{pmatrix}\begin{pmatrix}x_1\\ x_2\\ x_3\\ x_4\end{pmatrix} + \begin{pmatrix}2ax_1^2\\ -4ax_1x_2\\ 0\\ 0\end{pmatrix}, \quad (15)$$

where $b=k\sqrt{4a^2-k^2}$. The dynamics, Eq. (15), consist of two noninteracting subspaces, a "plane wave plane" (x_1x_2-plane) and a "sideband plane" (x_3x_4-plane). We see that trajectories which start off the x_1x_2-plane will settle onto it because $k>2a$. Physically, this implies that any spatial modulation of a plane wave will settle down to a plane wave state. This is also a property of the NLS. The resonant terms in Eq. (15) were those identified by performing a normal form analysis (see, for example, [25], for a discussion of normal form analysis).

Earlier, we mentioned that the normal form can give spurious roots. To demonstrate this, we will compare the dynamics on the plane-wave plane of the current problem (15) with the two-dimensional problem from [19]. Both problems describe the exact same physical situation, but because different coordinates are used to describe each problem (action-angle coordinates are used in the two-dimensional problem) they each have different quadratic terms in their dynamics. The fact that we truncate the normal form to quadratic order implies that the fixed points that are found depend on what terms appear in F_2. We begin by looking at the dynamics of the two-dimensional problem:

$$\begin{pmatrix}\dot{x}_1\\ \dot{x}_2\end{pmatrix} = \begin{pmatrix}-\epsilon_R & 2\\ 0 & -\epsilon_R\end{pmatrix}\begin{pmatrix}x_1\\ x_2\end{pmatrix} + \begin{pmatrix}0\\ -\epsilon_R a^2 x_1^2\end{pmatrix}. \quad (16)$$

Other than the target, which is at the origin, the fixed points of Eq. (16) are

$$x_1 = \frac{\epsilon_R}{2a}, \quad x_2 = -\frac{\epsilon_R^2}{4a^2}. \quad (17)$$

The above fixed point corresponds to a saddle. Next, we look at the plane-wave dynamics of Eq. (15):

$$\begin{pmatrix} \dot{x}_1 \\ \dot{x}_2 \end{pmatrix} = \begin{pmatrix} -\epsilon_R & 1 \\ 0 & -\epsilon_R \end{pmatrix} \begin{pmatrix} x_1 \\ x_2 \end{pmatrix} + \begin{pmatrix} 2ax_1^2 \\ -4ax_1x_2 \end{pmatrix}. \tag{18}$$

The fixed points of Eq. (18), other than the target, are

$$x_1 = \frac{\epsilon_R}{2a}, \quad x_2 = 0 \tag{19}$$

and

$$x_1 = -\frac{\epsilon_R}{4a}, \quad x_2 = -\frac{3\epsilon_R^2}{8a}. \tag{20}$$

If one inserts Eq. (19) into Eq. (15) (with $x_3 = x_4 = 0$) one will find that Eq. (19) behaves like a saddle point. Hence it could be a point of interest (a saddle point that bifurcates with the target as $\epsilon_R \downarrow 0$). However, no such point appears in the two-dimensional system and both sets of equations describe the same system. This leaves us with the question of whether or not Eq. (19) is a new fixed point of the four-dimensional system, or is it simply a spurious root produced by a low-order truncation of the normal form.

The fixed points (19) and (20) are also fixed points of Eq. (15) when $x_3 = x_4 = 0$. We can also see that each of these fixed points come in the form: $x_1 = \epsilon_R \alpha_1$, $x_2 = \epsilon_R^2 \alpha_2$, and $x_3 = x_4 = 0$. Using the normal form transformation, this translates to looking for fixed points which lie in the XY-plane ($U = V = 0$) that scale like ϵ_R in the Y-direction and ϵ_R^2 in the X-direction. Note that the origin is the target. We will insert these scalings into the original equations, (12), to find the location of the fixed points. Then, our coordinate tranformation becomes $x = a + \epsilon_R^2 \alpha_2$, $y = \epsilon_R \alpha_1$, and $u = v = 0$. We plug these scalings into Eq. (12) and solve for α_1 and α_2 to find the location of the fixed point. We find:

$$y_S = -\frac{\epsilon_R}{2a} + O(\epsilon_R^2),$$

$$x_S = a - \frac{\epsilon_R^2}{4a^3} + O(\epsilon_R^3),$$

$$v_S = 0,$$

$$u_S = 0, \tag{21}$$

as the position of the only fixed point near the target to leading order in ϵ_R. Hence we see that Eq. (20) is, indeed, a spurious root. While verification of the nature of Eq. (20) is simple in this case, in later cases (such as Circle 3, below), solution of the original dynamics may not be possible. Next, we need to find the linear term of the dynamics of Eq. (12) linearized about the fixed point. The linearized dynamics will give us the nature of the fixed point. Linearizing Eq. (12) about the fixed point (using, for example, $x = x_S + X, X \ll 1$) gives

$$\begin{pmatrix} \dot{Y} \\ \dot{X} \\ \dot{V} \\ \dot{U} \end{pmatrix} = \begin{pmatrix} -3\epsilon_R & 4a^2 - \frac{5\epsilon_R^2}{2a^2} & 0 & 0 \\ -\frac{\epsilon_R^2}{2a^2} & \epsilon_R & 0 & 0 \\ 0 & 0 & -3\epsilon_R & 4a^2 - k^2 - \frac{5\epsilon_R^2}{2a^2} \\ 0 & 0 & k^2 - \frac{\epsilon_R^2}{2a^2} & \epsilon_R \end{pmatrix} \times \begin{pmatrix} Y \\ X \\ V \\ U \end{pmatrix} + \cdots, \tag{22}$$

where we ignore terms $O(\epsilon_R^3)$ and higher, as well as terms $O(X^2)$ and higher. To leading order in ϵ_R, the eigenvalues of the matrix in Eq. (22) are

$$\lambda_1 = (-1 + \sqrt{2})\epsilon_R + O(\epsilon_R^3),$$

$$\lambda_2 = (-1 - \sqrt{2})\epsilon_R + O(\epsilon_R^3),$$

$$\lambda_3 = \frac{k}{a^2}\sqrt{4a^2 - k^2} - \frac{\epsilon_R}{2a^2} + O(\epsilon_R^2),$$

$$\lambda_4 = -\frac{k}{a^2}\sqrt{4a^2 - k^2} - \frac{\epsilon_R}{2a^2} + O(\epsilon_R^2). \tag{23}$$

Likewise, the eigenvectors of Eq. (22) to leading order in ϵ_R are

$$v_1 = \left(1, \frac{2 + \sqrt{2}}{2a^2}\epsilon_R, 0, 0\right),$$

$$v_2 = \left(1, \frac{2 - \sqrt{2}}{2a^2}\epsilon_R, 0, 0\right),$$

$$v_3 = \left(0, 0, 1, k\sqrt{4a^2 - k^2} - \frac{2\epsilon_R}{k^2}\right),$$

$$v_4 = \left(0, 0, 1, -k\sqrt{4a^2 - k^2} - \frac{2\epsilon_R}{k^2}\right), \tag{24}$$

where like subscripts denote eigenvalue-eigenvector pairs. Hence we see that the point is a stable spiral [in the (3,4), i.e., u and v, directions] and a degenerate saddle [in the (1,2)-plane, i.e., xy-plane]. Since we know the location of the fixed point and its stability, we can now visualize parts of the phase space of Eq. (12) near the target. Since the target and the saddle lie solely in the xy-plane, we will look at only this plane in the phase space as is illustrated in Fig. 1. In Fig. 1 we see that in this plane, the target, O, has a teardrop shaped basin of attraction in this plane, a hallmark of a Takens-Bogdanov bifurcation. The saddle point, S, given by Eq. (21) lies near the target. One piece of the saddle's unstable mani-

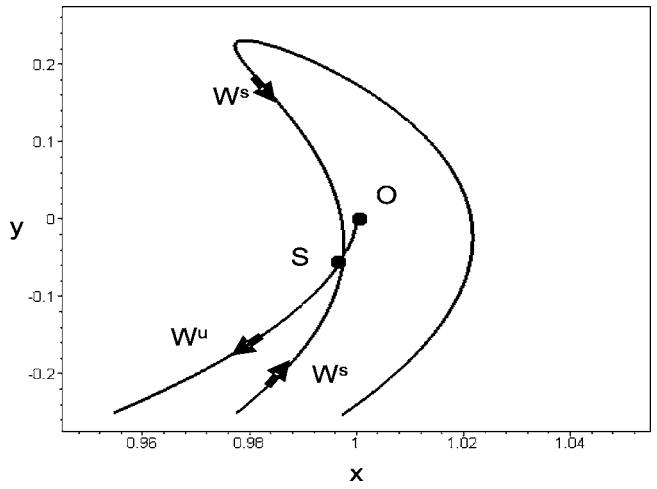

FIG. 1. The xy-plane in the phase space of Eq. (12) near the target.

fold (W^u) goes to the target while the other piece goes to a spiral (not shown) in the xy-plane. The stable spiral represents a low-amplitude, $O(\epsilon_R)$, plane wave.

We see that the two eigenvectors in the xy-plane are becoming degenerate (parallel) as $\epsilon_R \downarrow 0$. Following our algorithm, we need to find the angle, θ, between those two eigenvectors (see Fig. 2), using the dot product of these two vectors. Once θ is found, we can use the triangle relation (see Fig. 2) to find σ_c:

$$\sigma_c \approx |y_S \theta| = \frac{\epsilon_R^2 \sqrt{2}}{4a^3}. \tag{25}$$

The scaling for the four-dimensional system when we target Circle 1 is the same as that in the two-dimensional problem.

In [19], we discussed how to improve our estimate (25) as well as compute the error terms by including more terms in

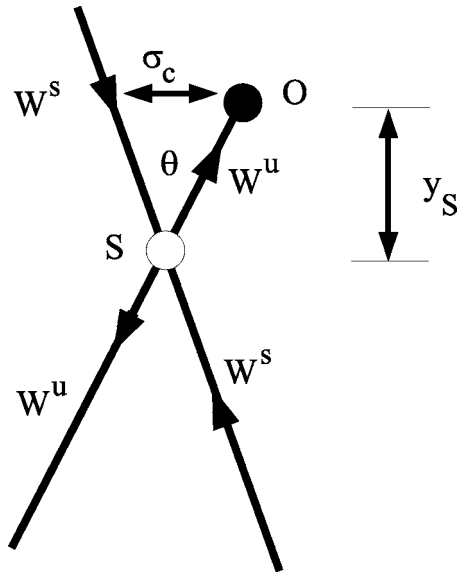

FIG. 2. An illustration of the xy-plane zoomed-in near the target.

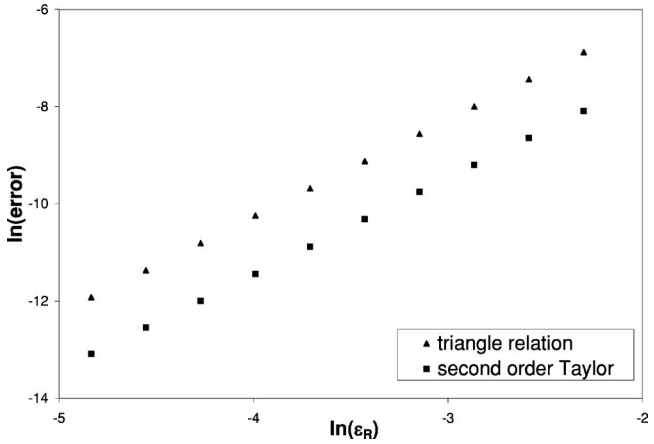

FIG. 3. The relative error of the triangle relation (triangle) and the polynomial approximation (squares).

the Taylor approximation of the stable manifold of the saddle. Note that the triangle relation gives an approximation of the linear term of the stable manifold's (W^s) Taylor series. In this problem, the stable manifold is three-dimensional (see the eigenvalue structure of the saddle). However, we are fortunate that the dynamics of the saddle (and the node) are normal and attracting in directions off of the xy-plane. Therefore we can reduce this problem to finding the one-dimensional curve of the stable manifold in the xy-plane. Finding an approximate equation for the stable manifold of the saddle is the same as finding an approximate equation for $x(y)$ near the saddle point. Therefore we are interested in solving

$$F(y;x) \equiv \frac{dx}{dy} = \frac{\epsilon_R(a-x) - 2y(x^2+y^2-a^2)}{-\epsilon_R y + 2x(x^2+y^2-a^2)} \tag{26}$$

for $x(y)$. The stable manifold will be the curve, $x(y)$, which passes through the saddle point in the direction of the saddle's stable eigenvector. We approximate the stable manifold in this plane with a quadratic polynomial, $x(y)$. The algebra here is straightforward and is presented in [26]. By Fig. 1, we can estimate the correction to Eq. (25) to be $\sigma_c \approx a - x(y=0)$,

$$\sigma_c = \frac{9}{32a^3}\epsilon_R^2 + O(\epsilon_R^4). \tag{27}$$

Figure 3 verifies this scaling. In Fig. 3, we have the relative error between Eqs. (25) and (27). Here, relative error is the absolute value of the difference between the "true" value of σ_c (found numerically) and those values of σ_c predicted by Eqs. (25) and (27). We see that the estimate of σ_c made by the triangle relation (triangles) is not as good as that made by the quadratic approximation (squares), as is expected. Further, we see that the quadratic approximation of the stable manifold converges a little quicker than the triangle relation. It is important to point out that the much easier computation of the triangle relation gives the correct scaling for σ_c in both ϵ_R and a (ϵ_R^2/a^3). The true value of σ_c is obtained by integrating Eq. (12) starting at the saddle in the direction of the

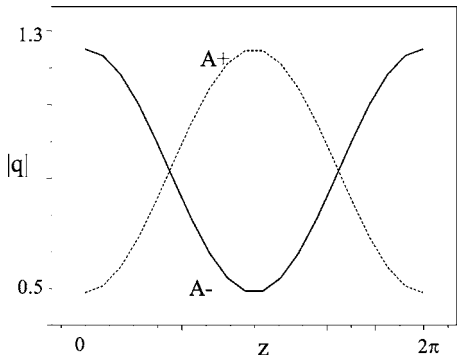

FIG. 4. A $|q|$ vs z profile of the attractors A_+ and A_-.

stable manifold backwards in time. The intersection of the stable manifold and the x-axis is approximately σ_c.

2. The case in which plane waves are modulationally unstable ($k>2a$)

As can be seen from the eigenvalue structure of Eq. (13), if $k<2a$ then the Circle 1 target is unstable if $\epsilon_R < k\sqrt{4a^2-k^2}$. This provides a threshold for control, the time scale for relaxation to the control target $[O(1/\epsilon_R)]$ must be faster than the exponential growth rate of the instability $(k\sqrt{4a^2-k^2})$. When ϵ_R is below the threshold $(k\sqrt{4a^2-k^2})$ then the system cannot be controlled to the target. When attempting to control the full PDE (5), a similar threshold will arise. In fact, when ϵ_R is below the threshold, two other attracting fixed points exist which we call A_+ and A_-. Algebraic expressions for the locations of A_+ and A_- are not easy to find. In the two-dimensional problem, these two attractors never appear as they exist off of the plane wave plane. Figure 4 shows the profile of $|q|$ vs. z at each one of these attractors. As $\epsilon_R \to k\sqrt{4a^2-k^2}$, A_+ and A_- collide at the point, $(y=0, x=a, v=0, u=0)$, and form the target. From Fig. 4 one can see that the "addition" of A_+ and A_- yields a plane wave (spatially uniform wave). For $\epsilon_R > k\sqrt{4a^2-k^2}$, the target is the sole attracting fixed point.

3. Summary of the Circle 1 problem

When $k>2a$, plane waves are modulationally stable and the interesting dynamics lie on the xy-plane. The noise threshold, σ_c, has similar scalings in ϵ_R and a as the two-dimensional problem. The analysis of the four-dimensional problem becomes more difficult than the two-dimensional problem due to the appearance of spurious roots in the normal form. However, this is fairly easily handled by using the scaling of the fixed points found from Eq. (15) to find the fixed points in the original dynamics (12). This step will not always be simple (see the Circle 3 problem below). Another new issue we must attend to in the four-dimensional problem deals with the modulational instability of plane waves. When ϵ_R is less than the linear growth rate the target is no longer viable. New attractors appear off of the plane wave plane, but bifurcate to form the control target as $\epsilon_R \to k\sqrt{4a^2-k^2}$. This provides one more necessary condition for the Circle 1 solution to be a viable control target.

B. Targeting Circle 2: C2=$(y,x,v,u)=(0,0,0,\sqrt{\frac{4}{3}(a^2+\frac{1}{2}k^2)})$

In this section, we will overview the results of the Circle 2 problem. For the algebraic details, the interested reader is referred to [26]. Similar to the Circle 1 problem, the Circle 2 problem can be broken up into two cases, one in which $k \neq a$ and one in which $k=a$. The analysis of the first case (when $k \neq a$) is similar to that of the Circle 1 problem, except that in this case the Takens-Bogdanov bifurcation occurs in the sideband (uv) plane. In the end, we find that $\sigma_c \approx O(\epsilon_R^2)$.

The more interesting case occurs when $k=a$. In this case, the normal form about the target is

$$\begin{pmatrix} \dot{x}_1 \\ \dot{x}_2 \\ \dot{x}_3 \\ \dot{x}_4 \end{pmatrix} = \begin{pmatrix} -\epsilon_R & 1 & 0 & 0 \\ 0 & -\epsilon_R & 0 & 0 \\ 0 & 0 & -\epsilon_R & 1 \\ 0 & 0 & 0 & -\epsilon_R \end{pmatrix} \begin{pmatrix} x_1 \\ x_2 \\ x_3 \\ x_4 \end{pmatrix} + \mathbf{F}_2(\mathbf{x}), \tag{28}$$

where x_1, x_2, x_3, and x_4 are proportional to V, U, Y, and X, respectively, and F_2 contains only quadratic terms. Note that the capitalized coordinates are the ones used to linearize the Circle 2 dynamics about the target (similar to the Circle 1 problem). It is clear that we have two Takens-Bogdanov bifurcations occuring; one in the plane wave plane, and the other in the sideband plane. This is different from the previous cases. We need to be cautious and determine the nature of the bifurcations in each plane. We are interested only in the case where a stable and an unstable pair of eigenvectors become degenerate as $\epsilon_R \downarrow 0$. Like the Circle 1 problem, Eq. (28) produces spurious roots. Using the scalings for the fixed points [obtained by Eq. (28)], we find that there is only one fixed point near the target. It turns out that this fixed point has one unstable direction and three stable ones. In the plane wave plane, two of the stable eigenvectors become degenerate in a Takens-Bogdanov bifurcation as $\epsilon_R \downarrow 0$. Hence this bifurcation is of no interest to us in terms of control. The other Takens-Bogdanov bifurcation, occuring in the sideband plane, has one stable and one unstable eigenvector becoming degenerate. This is the bifurcation of interest. By continuing the analysis on the sideband plane, we find that $\sigma_c \approx O(\epsilon_R^2)$.

C. Targeting Circle 3: C3=$(y,x,v,u)=(0,\sqrt{(k^2+a^2)/5},0,\sqrt{2(4a^2-k^2)/15})$

In this section, we will overview the results of the Circle 3 problem. For a detailed algebraic analysis, the interested reader is referred to [26]. In this problem, the Takens-Bogdanov bifurcation is not obvious in the physical coordinates. This becomes clear when we transform to coordinates that place the linear dynamics in Jordan canonical form (i.e., "normal form coordinates"). The bifurcation still occurs on a plane, however, the physical interpretation of the plane is not as simple as in the other two problems. This is because the solution does not lie solely on the xy- or uv-plane. The normal form of the dynamics linearized about the target gives many spurious roots. However, in this problem we cannot find the true roots of the Circle 3 dynamics analytically (i.e., the roots of the controlled dynamics in the physical coordi-

nates), even with the insight into the root's scaling given by the normal form analysis. However, we can still use insights obtained from the other two problems and numerical methods to verify the presence of the second fixed point and its saddle nature, then proceed to estimate σ_c as before. Such a blending of numerical and analytical techniques will be required as the dimensionality of our control problems increase. In the end, we find that for the Circle 3 problem, $\sigma_c \approx O(\epsilon_R^2)$.

IV. CONCLUSIONS

When attempting to control a high-dimensional integrable Hamiltonian system to one of its solutions, a high-dimensional Takens-Bogdanov bifurcation can occur. In most of our NLS examples, only a low-dimensional Takens-Bogdanov bifurcation occurred. This is because the solutions we are targeting have a saddle structure to them unlike Eq. (4) which assumes a generic solution. In each of the cases above, the wave number, k, determines whether the target solution is a saddle or a node. This physically makes sense for the NLS since the wave number determines whether or not plane waves are modulationally stable. When targeting Circles 1 and 2, we found that the Takens-Bogdanov bifurcation occurred either in the xy-plane (for Circle 1) or the uv-plane (for Circle 2). This is due to the fact that the target lies solely in its respective plane. In these problems, the Takens-Bogdanov bifurcation is obvious in the physical (y,x,v,u) coordinates. The Takens-Bogdanov bifurcation that occured in the Circle 3 problem did not occur in either of those two planes. This is because the Circle 3 target does not lie on either plane alone. However, the presence of the Takens-Bogdanov bifurcation is clear when our coordinates are chosen such that the linear dynamics are in Jordan canonical form.

Finding the noise thresholds for the above systems involved a nontrivial extension of the algorithm developed in [19]. After determining the stability conditions for each target, we had to identify the nature of the Takens-Bogdanov bifurcation. When $k=a$ for the Circle 2 target, we had two Takens-Bogdanov bifurcations occurring. The Takens-Bogdanov bifurcation of interest needed to be identified by studying the stability of the saddle point. Also, obtaining the location of the saddle point was not as straightforward as in the two-dimensional problem. We found that the normal form gave spurious roots due to the truncation at quadratic order. While some of the roots were spurious, the scalings of the roots could be used in the original equations to find the position of the actual fixed points. In the Circle 3 problem, this could not be done analytically and therefore numerical methods needed to be used. We expect that as the dimensionality of the system increases, we will need to rely more on numerical techniques. In each of the above cases, a blind application of the algorithm from [19] could have produced erroneous results and therefore the algorithm needed to be modified.

ACKNOWLEDGMENTS

This work was supported by the NSF-DOE Program in Basic Plasma Physics and the USDOE Office of Fusion Energy Sciences.

[1] Y. C. Lai, M. Ding, and C. Grebogi, Phys. Rev. E **47**, 86 (1993).
[2] Y. C. Lai, T. Tel, and C. Grebogi, Phys. Rev. E **48**, 709 (1993).
[3] Y. C. Lai, Phys. Lett. A **221**, 375 (1996).
[4] Y. Zhang, S. Chen, and Y. Yao, Phys. Rev. E **62**, 2135 (2000).
[5] E. M. Bollt and J. D. Meiss, Physica D **81**, 280 (1995).
[6] O. J. Kwon, Phys. Lett. A **258**, 229 (1999).
[7] J. H. Yim, Y. Kim, and O. J. Kwon, J. Korean Phys. Soc. **28**, 561 (1995).
[8] E. M. Bollt and J. D. Meiss, Phys. Lett. A **204**, 373 (1995).
[9] R. Haberman and E. K. Ho, J. Appl. Mech. **62**, 941 (1995).
[10] Y. Zhang and Y. Yao, Phys. Rev. E **61**, 7219 (2000).
[11] H. Xu, G. Wang, and S. Chen, Phys. Rev. E **64**, 016201 (2001).
[12] Y. L. Bolotin, V. Yu. Gonchar, A. A. Krokhin, A. Tur, and V. V. Yanovsky, Phys. Rev. Lett. **82**, 2504 (1999).
[13] C. G. Schroer and E. Ott, Chaos **7**, 512 (1997).
[14] U. Vaidya and I. Mezić, Physica D **189**, 234 (2004).
[15] A. Litvak-Hinenzon and V. Rom-Kedar, Nonlinearity **15**, 1149 (2002).
[16] A. Litvak-Hinenzon and V. Rom-Kedar, Physica D **164**, 213 (2002).
[17] I. Mezić, Physica D **154**, 51 (2001).
[18] I. G. Polushin, Int. J. Robust Nonlinear Control **11**, 253 (2001).
[19] C. W. Kulp and E. R. Tracy, Phys. Rev. E **70**, 016205 (2004).
[20] A. R. Bishop, M. G. Forest, D. W. McLaughlin, and E. A. Overman II, Phys. Lett. A **144**, 17 (1990).
[21] E. R. Tracy and H. H. Chen, Phys. Rev. A **37**, 815 (1988).
[22] V. I. Arnold, *Mathematical Methods of Classical Mechanics* (Springer-Verlag, New York, 1978).
[23] E. R. Tracy and X.-Z. Tang, Phys. Lett. A **242**, 239 (1998).
[24] J. Guckenheimer and P. Holmes, *Nonlinear Oscillations, Dynamical Systems and Bifurcations of Vector Fields* (Springer-Verlag, New York, 1993).
[25] S. Wiggins, *Introduction to Applied Nonlinear Dynamical Systems and Chaos* (Springer-Verlag, New York, 1990).
[26] C. W. Kulp, Ph.D. thesis, The College of William and Mary (unpublished).
[27] L. Friedland and A. G. Shagalov, Phys. Rev. E **71**, 036206 (2005).